Available online at www.sciencedirect.com
SCIENCE DIRECT®
International Journal of Pharmaceutics 253 (2003) 133–144
international journal of pharmaceutics
www.elsevier.com/locate/ijpharm

Evaluation of gliadins nanoparticles as drug delivery systems: a study of three different drugs

C. Duclairoir [a], A.-M. Orecchioni [b,*], P. Depraetere [c], F. Osterstock [d], E. Nakache [a]

[a] *Equipe Polymères-Interfaces, ISMRa, LCMT UMR 6507, 14050 Caen Cedex, France*
[b] *Université de Rouen, UFR de Médecine et Pharmacie, 76183 Rouen, France*
[c] *Laboratoire de Pharmacie Galénique, Bd Becquerel, Hérouville St Clair, 14032 Caen Cedex, France*
[d] *ESCTM/CRISMAT, UMR 6508, ISMRa, 14050 Caen Cedex, France*

Received 15 February 2002; received in revised form 2 December 2002; accepted 11 December 2002

Abstract

In this paper, biopolymer nanoparticles are studied, which unlike many synthetic carriers used for controlled release, are biocompatible and biodegradable systems. Gliadins nanoparticles are obtained by a desolvatation method, also known as drawning-out precipitation. These particles have been shown to be interesting as drug release systems for all-*trans*-retinoic acid. The aim of this paper was to study the influence of the polarity of different drugs on nanoparticle characteristics such as size and drug loading efficiency. Three drugs of three different polarities were studied: the hydrophobic Vitamin E (VE), the slightly polar mixture of linalool and of linalyl acetate (LLA) and the cationic amphiphilic benzalkonium chloride (BZC). This comparative work shows that the amount of the entrapped VE and LLA is higher than that of the cationic BZC, confirming a strong interaction between gliadins and apolar compounds, due to the apolarity of the proteins. This interaction results in a low diffusion coefficient and a partition coefficient in favour of gliadins, resulting in a low permeability coefficient. The drug release kinetics of two substances, LLA and BZC, are observed, in showing a burst effect, then a diffusion process, which can be modelled assuming that the particles are homogeneous spheres.

Keywords: Nanoparticles; Gliadins; Vitamin E; Linalool; Linalyl acetate; Benzalkonium chloride

1. Introduction

Drug delivery systems are interesting formulations to prevent numerous drawbacks related to the drug itself, for example by decreasing its degradation rate. In such a dosage form, the drug is gradually released unlike all conventional formulations. Several carriers have been studied in the last decades, among them, liposomes, vesicles, films, sponges, simple or complex emulsions, and particles. These last named delivery systems are found as spheres or capsules for core/shell particles. Particles are classified as microparticles for micron-sized systems and as nanoparticles for sub-micronic systems (Thies, 1996). Most of them are derived from synthetic polymers and some from biopolymers (Nakache et al., 2000). Recently, gliadins, extracted from wheat gluten, have been used to elaborate nanoparticles (Ezpelleta et al., 1996; Duclairoir et al., 1999). As biopolymers, gliadins do not present the common drawbacks of synthetic materials, related to the presence of monomer or initiator residues (Chasin and Langer,

* Corresponding author. Tel.: +33-1-46612713; fax: +33-1-46612713.
E-mail address: oreccam@wanadoo.fr (A.-M. Orecchioni).

0378-5173/02/$ – see front matter © 2002 Elsevier Science B.V. All rights reserved.
doi:10.1016/S0378-5173(02)00701-9

1990). Their biocompatibility is assumed and, as plant proteins, they are recognized as prion-free unlike animal proteins. Besides gliadins are hydrophobic and slightly polar (Bigelow, 1967; Popineau and Denery-Papin, 1995). Consequently, they are able to interact with skin keratin (Teglia and Secchi, 1994). Thus, gliadin systems seem to have promise in the development of topical formulations. Moreover, previous work has shown that the preparation of gliadin particles can be easily performed by simple coacervation method (Ezpelleta et al., 1996). The obtained gliadins systems are spherical and submicron-sized, thus are nanoparticles. They proved to be interesting delivery systems for all-*trans*-retinoic acid (RA).

In this study, three drugs of different polarity have been entrapped in such gliadins nanoparticles. There are the hydrophobic Vitamin E (VE), the slightly polar linalool/linalyl acetate mixture (LLA), and the amphiphilic and cationic benzalkonium chloride (BZC), with dielectric constants (ε) respectively of 4, 8 and 45 (Maryott and Smith, 1951).

α-Tocopherol (Vitamin E) is known as a strong antioxidant or nitrosamine blocker to prevent built up of cellular peroxides (Idson, 1992; Marty and Wepierre, 1994). For instance, free radicals may promote skin damages such as premature skin aging (Epstein, 1983), skin fragility and even skin cancers such as melanoma (Sober, 1987) related to a decrease in cellular immunity of the skin. VE is known to delay the progression of aging (Wester and Maibach, 1997), to have skin moisturising properties (Mayer et al., 1993) and emolliency properties (Tamburic et al., 1999; Marty, 1998). However, VE is degraded by oxygen and must be carefully protected from light, heat and contact with air when it is used in formulations and dosage forms. To overcome these drawbacks, liposome dosage forms were formulated (Kagan et al., 1992; Koga and Terao, 1996). Nanoparticulate carriers from bioacceptable macromolecules, particularly gliadins, are also interesting system for controlled drug release. They are able to interact with epidermal keratin due to their being rich in proline (Teglia and Secchi, 1994).

Linalool and linalyl acetate are the major components of aromatic lavender essential oils, frequently used in aromatherapy. Moreover, linalool and linalyl acetate give antibacterial and antifungal properties (Lis-Balchin and Hart, 1999) to the formulations. In dermatologic formulations, for instance, their use may irritate the patient's skin. Gliadins encapsulation could be a fruitful method for LLA formulation. The coupling of gliadins proline, which allows a powerful attraction to the skin keratin, and of the gradual and controlled LLA release, potentially avoids all the potential drawbacks of the drug and even improves LLA disposition.

BZC is a cationic surfactant often used as antiseptic, bactericide (Patterson, 1956), spermicide (Aubeny et al., 2000) or virucide (Wainberg et al., 1990). Some original formulations of this drug, better known as Zeriphian®, are on the market. There are capsules (Wainberg et al., 1990) and vaginal Protectaid® sponges (Psychoyos et al., 1993). But the medication can promote some allergies followed by mucous lesions (Dhillon et al., 1982). Thus, a dosage form such as gliadins nanoparticles could be a good alternative and could avoid lesions promoted by the irritant BZC and, even, could improve the therapeutic dosage by delaying the delivery.

This paper reports on the characterization, entrapment and release studies on the novel drug delivery systems.

2. Materials and methods

2.1. Materials

Gliadins were extracted and purified by Y. Popineau (LBTP, INRA, Nantes, France). α-Tocopherol (VE) and benzalkonium chloride (BZC) were obtained from Sigma (St. Louis, MO, United States). The aromatic extract (LLA) was provided by Euracli (France). Synperonic® PE F68 was furnished by ICI surfactant (Cleveland, United Kingdom). All the aqueous solutions were prepared with ultrapure water (Milli Q Plus, Millipore, Molsheim, France). Ethanol and sodium chloride were of analytical grade and obtained from Prolabo (Paris, France).

For VE estimation, methanol (HPLC grade) was obtained from Carlo Erba Reagenti (Val de Reuil, France) and decane (spectroscopic grade) from Acros Organics (Geel, Belgium).

LLA quantification was performed using linalool from Touzart and Matignon (Paris, France) and

pentane (spectroscopic grade +99%) from Acros Organics (Geel, Belgium).

BZC content was estimated using chloroform (synthetic grade 99.9%) from SDS (Peypin, France), sulphuric acid (analytical grade 96%) from Carlo Erba Reagenti (Val de Reuil, France), sodium hydroxide 0.1N standard solution from Distrilab (Caen, France), sodium dodecylsulfate or sodium laurylsulfate (SDS, analytical grade 99%) from Sigma (St. Louis, United States), benzethonium chloride 0.00398N standard solution from Prolabo (Paris, France), Patent blue VF or blue disulfine VN 150 from Acros Organics (Geel, Belgium), phenolphthalein from Prolabo (Paris, France), and dimidium bromide from Acros Organics (Geel, Belgium).

2.2. Gliadins extraction and purification

Gliadins were extracted from a common wheat flour (Hardi variety) (Larré et al., 1991). Briefly, gluten was freeze dried, ground in a refrigerated grinder and defatted by two extractions with dichloromethane (gluten/solvent ratio: 1/10) for 2 h at 20 °C. After filtration and residual solvent evaporation under reduced pressure, samples of dried powder were stored in an ethanol/water mixture (70/30, v/v) for 4 h at 20 °C. The soluble fractions were then dialysed against distilled water and finally freeze dried.

For this study, the gliadins extract consists of four fractions: α-, β-, γ- and ω-gliadins. The fractions are classified due to their hydrophobicity and to their mean molar mass. This extract has been characterized by high performance liquid chromatography-reverse phase (HPLC-RP). It contains 53.7% of α/β-gliadins, 39.9% of γ-gliadins and 6.4% of ω-gliadins.

2.3. Drug quantification

The choice of the three drugs (VE, LLA and BZC) was made according to their polarity difference. In consequence, their solubility behaviour differs for a given solvent.

VE could be easily characterized by its specific absorption at 295 nm by UV-spectrophotometry. VE quantification is assayed by HPLC-RP at room temperature using a photodiodes array detector (Waters 600, Millenium 32 software, Waters, Milford, United States) at 295 nm, and a 250 mm × 3 mm Nucleosil® 100-5, packed with C_{18} column (Macherey Nagel, Düren, Germany).

The medium containing LLA is not compatible with a gas phase chromatography (GPC) analysis used to quantify the perfume. First of all, the LLA is extracted from the sample by pentane. LLA solution and pentane are mixed in equal proportion. The LLA transfer is known taking into account its partition coefficient between the two solvents. To determine this partition coefficient, a known LLA quantity is dissolved in aqueous and ethanolic media. This medium is mixed with an equivalent volume of pentane. Then the LLA concentration is quantified in pentane. After collection of the aqueous phase, it is blended with the same volume of pure pentane. The LLA quantification is assayed in pentane. It is repeated until there are no remaining LLA traces in the pentane. The LLA partition coefficient between water and pentane was calculated as a function of extraction number, the initial LLA concentration in the aqueous phase and the experimental LLA concentrations in pentane. When the extraction is completed, 5 μl of the extracted solution is analysed by GPC (Varian 3300 GC-FID, United States) equipped with a flame ionisation detector and an apolar DB 5 column (Scientific Glass Engineering, Australia). The LLA content is measured by the quantification of linalyl acetate and linalool, which are respectively 35.7 and 39.7%.

The T73-258 and T73-320 AFNOR specifications have been adapted to perform the BZC titration. In fact, this quaternary ammonium is a cationic surfactant. Its titration consists of neutralisation by an anionic surfactant, the sodium laurylsulfate (SDS) in a biphasic water/chloroform system in the presence of colour indicators mixture (ethanolic solution of dimidium bromide 0.8% w/v and Patent Blue VF 0.4% w/v). During the neutralisation, a colour indicator salt is formed and confers pink colour to the organic phase. After complete BZC neutralisation, a BZC excess transfers the indicator salt from the organic phase to the aqueous one, which becomes blue and the organic fades up.

2.4. Preparation of drug loaded gliadins nanoparticles

The gliadins nanoparticles were prepared by a desolvatation method described elsewhere (Ezpelleta

et al., 1996; Duclairoir et al., 1999). In the case of VE, to prevent its degradation, the nanoparticle procedure has to be performed in the dark, under a nitrogen flow. Proteins were dissolved in an ethanol/water mixture (62/38, v/v) at 25 °C; the resulting solution was filtered through a 0.1 μm pore sized membrane. Various amounts of drug dissolved in ethanolic solutions were then added to the previous gliadins solution. The nanoparticle formation occurred when 20 ml of this solution were poured into a 0.9% w/v NaCl/water solution containing Synperonic® PE/F 68 (0.5%, v/v) as a stabiliser, at 25 °C, under stirring (500 rpm). The organic solvent was evaporated under reduced pressure, and the resulting suspension was centrifuged (20 000 rpm or 34 900 × g, 15 min). The supernatant was removed and, after three washes in ultra pure water, the loaded pellets were freeze dried and stored at 4 °C in the dark.

2.5. Physicochemical characterization

The size of the nanoparticles was characterized by scanning electron microscopy (Jeol, T330A, Japan).

The surface properties of the nanoparticles, loaded and non-loaded, were analysed by determining their zeta potential in a unimillimolar KNO_3 solution at room temperature. The nanoparticles were observed in very diluted conditions by a Sephy Zetaphorimeter III (Sephy, Limours, France).

The thermogram of nanoparticles, loaded and non-loaded, were obtained using differential scanning calorimetry (DSC) using a Perkin-Elmer DSC7 apparatus (Uberlingen, Germany) between −50 and 250 °C. The temperature gradient was 40 °C min^{-1}.

2.6. Drug loading

In order to measure the drug loading, around 1 mg of gliadins nanoparticles containing different amounts of drug was digested in 10 ml of the ethanol/water mixture (62/38, v/v) at 25 °C. The drug content C_1 was tested by the adequate analysis method according to the drug (Section 2.3). For VE, the experiments were performed in the dark under a nitrogen flow, as explained in Section 2.3.

The non-encapsulated drug remaining in the supernatant after the first centrifugation C_2 was also estimated.

With these two data, the drug loading (payload) was calculated as the entrapped drug in nanoparticles/gliadins nanoparticles yield ratio

$$\text{Payload (\%)} = \frac{C_1\ (\text{mg})}{\dfrac{\text{gliadins nanoparticles}}{\text{yield (mg)}}} \times 100 \qquad (1)$$

and the entrapment efficiency was calculated as the drug amount in particles/initial drug content ratio

$$\text{Entrapment efficacy (\%)} = \frac{C_1\ [\text{amount of drug in nanoparticles (mg)}]}{(C_1 + C_2)\ [\text{initial drug content (mg)}]} \times 100 \qquad (2)$$

For comparison of the different entrapped drugs, the dimensionless entrapment efficiency is adequate. But to simplify the comparison between drugs, an optimal drug concentration has been defined as the best compromise between the payload and the entrapement efficiency. This optimal drug concentration is the drug/gliadins ratio obtained at the intersection of payload and entrapment efficiency curves versus drug/gliadins ratio.

2.7. In vitro drug release

About 1 mg of gliadins nanoparticles containing X drug mg gliadins mg^{-1} were resuspended in a release medium under stirring.

In the case of VE, the release profile was performed three times by resuspending 10.1 mg of 824.0 VE μg gliadins mg^{-1} nanoparticles in 10 ml of decane. This solvent has been chosen because of its VE affinity, like most organic solvents. The solubility parameter of gliadins and of decane are respectively 34.5 (Duclairoir et al., 1998) and 19.0 MPa$^{1/2}$ (Barton, 1991). Considering such a difference of solubility parameters, the decane is not able to solubilize the gliadins nanoparticles and even to modify their surface. The release study was performed under nitrogen and in the dark in order to prevent VE loss.

For the BZC release, 741.5 mg of 550.3 BZC μg gliadins mg^{-1} nanoparticles were resuspended in 70 ml of ultrapure water at 25 °C. This release study has been replicated twice. The choice of water has been motivated by its inability to dissolve the gliadins nanoparticles and its ability to solulize BZC.

For each, the medium was then maintained in a release cell at 25 ± 0.2 °C. This original cell is constituted by a double shell leading to an efficient thermostating and by an access allowing easy collecting of aliquots exempted of nanoparticles by filtration through a 0.1 μm pore sized membrane. Aliquots of 100 and 700 μl have been collected respectively for VE during 120 h and for BZC during 150 h. After each sample collection at successive time intervals, t, an equal amount of thermostated release medium was introduced into the system. Thus, during the whole release, the nanoparticles concentration remained unchanged. The released drug amount, M_t, was evaluated, for each sample, by the adequate analysis technique as regards to the drug. Then the in vitro release is found using the plot of M_t/M_0 versus the time t with M_0 the effective drug loaded amount in the nanoparticles, expressed as "X drug mg gliadins mg^{-1}".

3. Results and discussion

3.1. Gliadins nanoparticles characterization

Gliadins, wheat gluten proteins, precipitate into nanoparticles by the desolvatation method known as "nanoprecipitation" (Stainmesse et al., 1995; Alonso, 1996), or coacervation, solvent displacement or drawning-out phenomenon (Mersmann, 1994).

These loaded and unloaded gliadins particles are spherical, as shown by scanning electron microscopy.

3.1.1. Size characterization

The mean volume–average diameters of loaded and unloaded nanoparticles are compiled in Table 1.

To decrease the experimental error on the mean value and to approach the real mean diameter, several micrographs of different places of the sample have to be analysed. The experimental error on the mean volume–average diameter is around 10%.

Although the experimental error due to the characterization method is more important than the difference between the diameters themselves, the number-average diameters obtained by SEM seem to increase with the drug polarity (ε, their dielectric constant) (Maryott and Smith, 1951), as shown Table 1. The more polar the drug, the larger the mean diameter is of loaded particles.

3.1.2. Zeta potential study

In Table 1, are mentioned the zeta potential of loaded particles and the drug polarity represented by its dielectric constant, ε, compiled in the literature. As anticipated, the unloaded nanoparticles are almost uncharged, as are the gliadins themselves.

The VE loaded nanoparticles have a similar ζ. It is explained considering the quite low VE dielectric constant ($\varepsilon = 4$). In the case of LLA, which is slightly polar ($\varepsilon = 8$), the charge is near zero (the error with such a technique is estimated around 3 mV).

The zeta potential of BZC loaded nanoparticles differs according to the drug amount in the particles. BZC is an ionized cationic surfactant ($\varepsilon = 45$). This difference could be explained by the presence of a fraction of the drug present at the particle surface, although the zeta potential does not increase as a function of the increasing loaded BZC concentration, as shown on Fig. 1.

In fact, after zeta potential change, a step value is reached around 25 mV. Such behaviour can be related

Table 1
Size characterization, zeta potential, glass transition temperature, entrapment efficiency and optimal drug concentration obtained for drug loaded nanoparticles according to the dielectric constant of the drug

Particles	Unloaded	VE loaded	LLA loaded	BZC loaded
ε	–	4	8	45
Mean diameter ±10% (nm)	900	900	930	950
Zeta potential (mV)	−1	−1	−1 to −4	20–40 varying with BZC concentration
T_g	145	134	130	110
Entrapment efficiency (%)	–	79.2	82.4	52.3
Optimal drug concentration (μg gliadins mg^{-1})	–	972.0	980.0	550.3

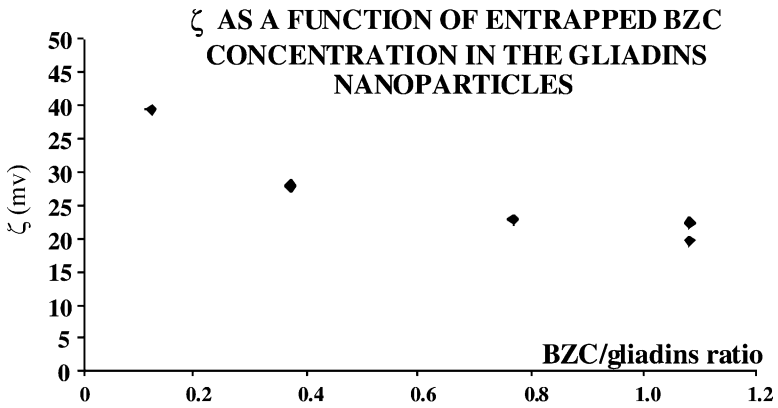

Fig. 1. Zeta potential of BZC loaded nanoparticles versus the drug entrapped concentration.

to the increased amount of charge number in the diffuse double layer inducing a shielding effect of the superficial charge decreasing the zeta potential value (Hunter, 1981).

3.1.3. DSC study

3.1.3.1. Unloaded nanoparticles. Gliadins and the surfactant (Synperonic® PE F68), as well unloaded gliadins nanoparticles were studied.

Gliadins, lead to a large glass transition temperature, T_g, around 165 °C. The surfactant thermogram shows a fusion peak at 52 °C. Then gliadins are blended with surfactant, a unique glass transition appears at 144 °C. The disappearance of the surfactant melting peak could be explained by its low amount or by perfect compatibility of the surfactant in the particle matrix. In any case, its presence is attested by decreasing glass transition temperature and can even be evaluated around 20%.

3.1.3.2. Loaded nanoparticles. Under the same conditions, thermogram of drug loaded nanoparticles show an unique transition corresponding to a glass transition. The corresponding T_g values are compiled in Table 1.

The thermogram of the drugs show no glass transition, but boiling peaks at 210 °C for VE, at 200 and 220 °C for LLA and at 36 °C for BZC. None of these peaks appear on the thermograms of drug loaded particles. For VE or LLA loaded particles, the obtained T_g are close and their difference is less than the experimental error of 10 °C usually attributed to DSC measurements. For BZC loaded nanoparticles, the T_g seems to decrease in the presence of drug. The BZC boiling point is lower than gliadins T_g and could explained this phenomenon. These results lead to the conclusion that the drug should be, at least, dispersed quite homogeneously inside the particle.

3.2. Drug entrapment study

Payload and entrapment efficiency are dependent on the drug/initial protein ratio.

3.2.1. VE entrapment

Fig. 2 represents the payload and the efficiency versus the VE/gliadins ratio. The encapsulated/initial VE payload increases from 0 to 82% and the encapsulated/initial VE efficiency decreases from 100 to 77%.

The optimal VE concentration is obtained for 972.0 VE μg gliadins mg^{-1}, with at least, an efficiency of 79.2%.

3.2.2. LLA entrapment

The partition coefficient of LLA between gliadins solvent and pentane is 0.630 and allows us to evaluate C_1, the effective LLA concentration contained in nanoparticles. After centrifugation, C_2, the remaining LLA concentration in the supernatant, is evaluated with the help of the partition coefficient of LLA between the supernatant and pentane estimated to be 0.204.

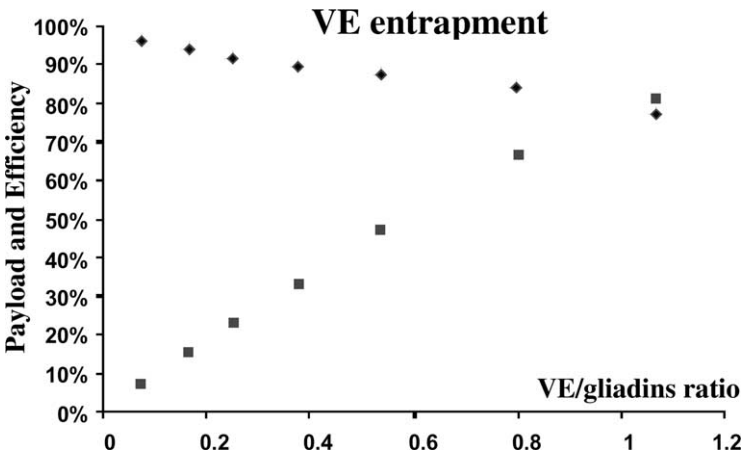

Fig. 2. Payload (■) and entrapment efficiency (◆) of VE loaded gliadins nanoparticles (experiment number $n = 3$).

On Fig. 3, the LLA payload and the LLA entrapment efficiency by gliadins nanoparticles are shown. The former increases from 0 to 94%, as the latter reduces from 100 to 76%.

The optimal LLA concentration corresponds to 980.0 LLA μg gliadins mg^{-1} with an efficiency of 82.4%.

3.2.3. BZC entrapment

BZC payload and BZC entrapment efficiency are plotted in Fig. 4. The efficiency decreases from 83 to 56% and the payload increases from 0 to 53%.

The optimal BZC concentration is achieved for 550.3 BZC μg gliadins mg^{-1} with an efficiency of 52.3%.

3.2.4. Comparison of entrapment capacity of gliadins nanoparticles

Table 1 shows the optimal drug concentration in nanoparticles and the corresponding efficiency for each drug. The close VE and LLA polarities result in similar optimum drug concentrations, including experimental error. Comparing the results of VE and BZC, molecules with a similar molar mass, indicate

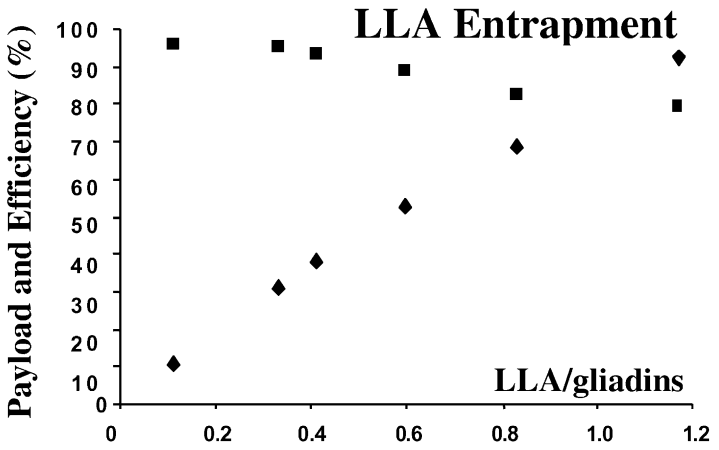

Fig. 3. Payload (■) and entrapment efficiency (◆) of LLA loaded gliadins nanoparticles ($n = 3$).

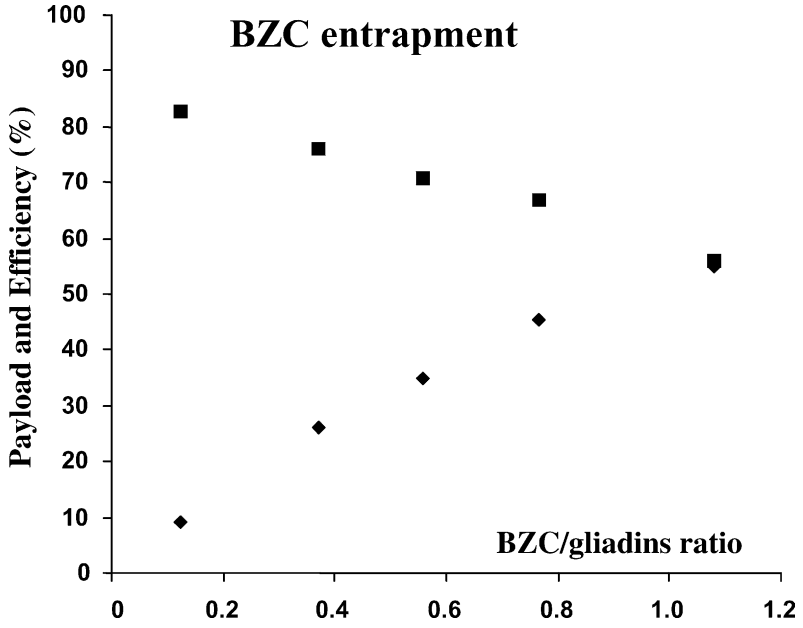

Fig. 4. Payload (■) and entrapment efficiency (◆) of BZC in gliadins nanoparticles ($n = 3$).

that the gliadins nanoparticles have more affinity for VE than for BZC, whose polarity is higher. VE is as apolar as the gliadins. Consequently, for any apolar substance, it could be assumed that gliadins nanoparticles would be able to entrap it with good results.

It can be noticed that BZC entrapment efficiency is reasonable, probably because of the hydrophobic chain of this amphiphilic molecule. These results confirm the low polarity of gliadins, whose ε is probably less than 8. Few results are described in literature concerning plant based nanoparticles and fewer about gliadins nanoparticles. The only interesting paper (Ezpelleta et al., 1996) is related to an entrapment study of all-*trans*-retinoic acid/gliadins. In this work, the highest ratio is just lower than 10%, the ratio used in our study is higher than 10%, but the corresponding entrapment efficiency are in concordance.

3.3. Drug in vitro release study

The release of two drugs, VE and BZC, has been studied. In fact, LLA should be studied under a controlled atmosphere and not in a liquid medium. Such differences between media used here does not allow an easy comparison to the other drugs.

3.3.1. VE in vitro release study

Gliadins nanoparticle preparations were tested for in vitro release in decane for about 120 h at 25 °C under nitrogen in the dark. During all the experimental period, no VE or no particle degradation was observed. The size and the morphology of nanoparticles have been measured before and after the release by SEM.

Fig. 5 shows that VE is released in two steps, characterized by an initial rapid release (under 1 h) which could be attributed to the adsorbed drug in the superficial zone of the spheres. This phenomenon is like a burst effect. The second releasing period shows a dependency on time and seems to be related to the drug diffusivity inside the matrix systems.

After roughly 3 h, at the break point between the two domains: burst effect and delayed release, the VE amount decreases in the release medium.

This disappearance might be explained by the following hypothesis. During the first period, both VE and surfactant (Synperonic® PE/F68) are released in the medium. This surfactant forms micelles at very low concentrations in decane (lower than 1 mg l^{-1}). Its amount in nanoparticles is evaluated around 20%. Thus, in the vicinity of the particles, its concentration could be sufficient to form micelles. These micelles

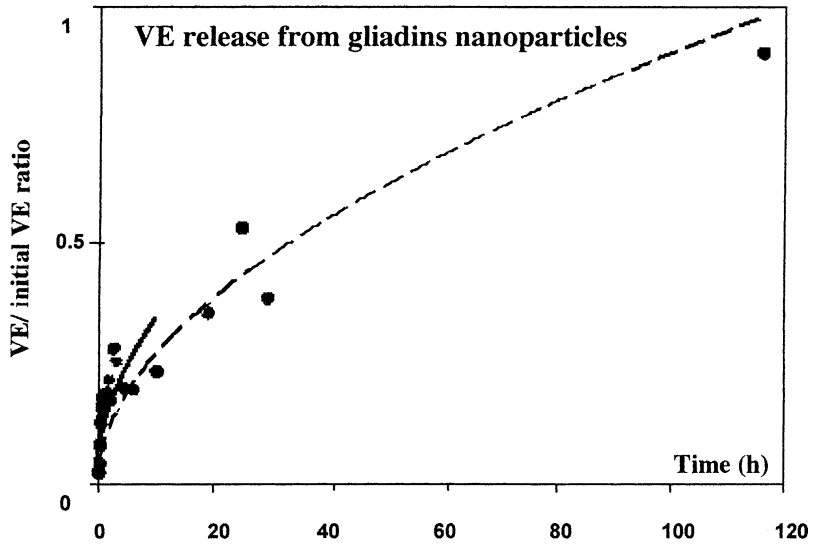

Fig. 5. VE release in decane from 824.0 VE μg protein mg^{-1} loaded nanoparticles at 25 °C fitted by short time model (—) and by medium time model (– – –) ($n = 3$).

are then able to encapsulate a part of the released VE, playing the role of drug-reservoirs. As VE is entrapped in the surfactant micelles, this should explain the observed fall in VE concentration in the release medium. During the second period, both VE and surfactant continue to be released in the medium.

In order to explain this release profile, an analytical model was applied. As shown by SEM, the particles are spherical. Assuming that the drug is uniformly distributed inside the delivery system, and that these remain stable during all the experimental period, it is known that (Washington, 1996)

$$\frac{M_t}{M_0} = 1 - \frac{6}{\pi^2}\sum_{n=1}^{\alpha}\left[\frac{1}{n^2}\exp(-n^2\pi^2\tau)\right] \quad (4)$$

where M_t is the amount of released drug at t time, and $(1 - (M_t/M_0))$ the released amount and t is given by

$$\tau = \frac{Dt}{R^2} \quad (5)$$

with D the drug diffusion coefficient through the particle and R the particle radius.

This relation is simplified for the first releasing period, i.e. the first few percent decays

$$\frac{M_t}{M_0} = 6\sqrt{\frac{\tau}{\pi}} \quad (6)$$

For the second period, the medium release time, this relation becomes

$$\frac{M_t}{M_0} = 6\sqrt{\frac{\tau}{\pi}} - 3\tau \quad (7)$$

For longer times, a simplification of Eq. (4) is

$$\frac{M_t}{M_0} = 1 - \frac{6}{\pi^2}\exp(-\pi^2\tau) \quad (8)$$

Sometimes, the release can be extensively described only by the short and long time model as shown by Guy et al. (1982).

The release has been fitted by this model for the first released drug and by the one for medium times, i.e. Eqs. (6) and (7). r^2, the correlation coefficient, is respectively 0.7321 and 0.9010. Obviously, the model of the first stage does not describe the experimental data. The difference could probably be explained by an underestimation of the burst effect by this diffusion model, and even, by experimental errors (less than 1%), but the hypothesis of drug-reservoir micelles could be an interesting complementary explanation.

For the second period, when the model for medium times is taken into account, the fit is close to the data. Then, the VE diffusion coefficient, D, through the gliadins nanoparticles can be determined; D/R^2 is $2.00 \times 10^{-4}\,s^{-1}$. As the average particle radius

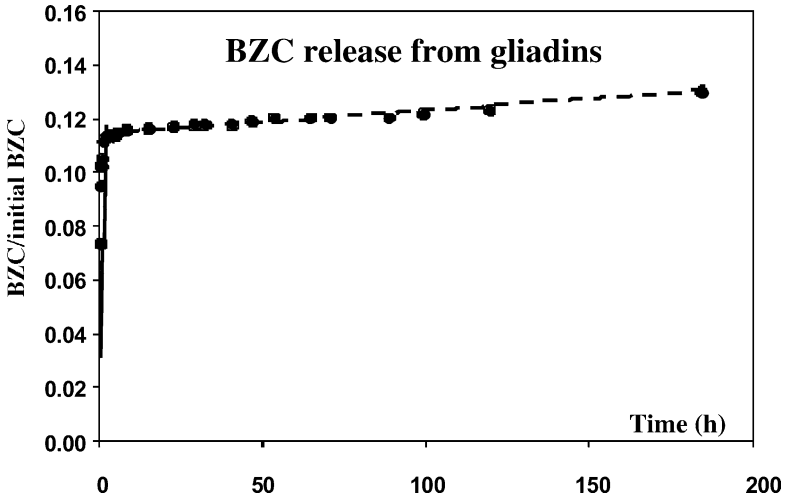

Fig. 6. BZC release in ultra pure water from 550.3 VE μg protein mg^{-1} loaded nanoparticles at 25 °C fitted by short time model (—) and by long time model (– – –) ($n = 3$).

is 0.45 μm, the VE diffusion coefficient through the gliadins nanoparticles is estimated around $4.1 \pm 0.1 \times 10^{-5}$ $\mu m^2\ h^{-1}$, i.e. $6.0 \pm 0.3 \times 10^{-20}$ $m^2\ s^{-1}$.

3.3.2. BZC in vitro release study

The in vitro release was performed at 25 °C during more than 150 h in ultra pure water. The BZC release profile is represented in Fig. 6.

In less than 30 min, a rapid release occurs until 11% of the total released amount. This first period can again be attributed to the drug desorption from the particle surface. Then the drug diffuses very slowly inside the nanoparticles; in fact, in more than 150 h, only a further 2% of the drug is released after the initial rapid release.

Once again, BZC kinetics is fitted by the model of a diffusion process in a homogenous sphere. SEM confirms that nanoparticles size remains constant before and after the drug release. After fitting, the data by Eqs. (6) and (8), i.e. short and long time models, r^2 values are respectively 0.5367 and 0.9669. Again, the data are not fitted properly by the short time model. As for VE release, the diffusion process in a homogenous sphere underestimates the "burst effect". It can be noticed that there is no BZC decrease, as for VE. It is not surprising, because no micelle formation can occur at such concentrations of the PE F68 surfactant in ultra pure water. Indeed in these conditions, the critical micellar concentration is 70 $g\ l^{-1}$.

The evaluation of BZC diffusion coefficient, D, is based on the long time model, for which D/R^2 equals $1.01 \times 10^{-4}\ s^{-1}$. As the mean particle diameter is 0.475 μm, the BZC diffusion coefficient through the gliadins nanoparticles is evaluated around $2.3 \pm 0.1 \times 10^{-5}$ $\mu m^2\ h^{-1}$, i.e. $6.0 \pm 0.3 \times 10^{-21}$ $m^2\ s^{-1}$.

3.3.3. Comparison of release studies

In organic phases, diffusion coefficients are usually about 10^{-9} $m^2\ s^{-1}$. Here the coefficients are clearly much lower (1.12×10^{-20} $m^2\ s^{-1}$ for VE and 6.36×10^{-21} $m^2\ s^{-1}$ for BZC). Thus, these results confirm that the drug is retained by the nanoparticle matrix Table 2.

The diffusion coefficient obtained using the homogeneous sphere model is different according to VE and BZC. This could be related to the different drug affinity for gliadins.

After 30 h, about 30% of encapsulated VE are released; on the other hand, after the same time, only 11% are released for BZC. This remark is verified more accurately after 120 h. Indeed, the release media are different for both drugs. However, the drug release process is related to the particle permeability, P, of each specific drug. In fact, this is a function of the drug

Table 2
Drug released percentage as a function of the release period and the drug diffusion coefficient through the loaded nanoparticles observed and compiled according to the drug

PA	Time (h)	Released drug (%)	Diffusion coefficient ($m^2\ s^{-1}$)
VE	1	13.2	1.12×10^{-20}
	30	30.6	
	120	70.1	
BZC	1	11.1	6.36×10^{-21}
	30	11.7	
	120	12.3	

diffusion coefficient, D_{drug}, across the particle and of the drug partition coefficient, K_{drug}, between the particle and the release medium as shown in Eq. (9).

$$P = \frac{K_{drug} \times D_{drug}}{d} \quad (9)$$

with d the distance covered by the drug through the nanoparticle, i.e. in this case, the particles radius. For both drugs, the nanoparticles radii are equivalent, thus d is similar and cannot explain the factor of two between the diffusion coefficients.

The only modified parameter between the two cases is K_{drug}. The most appropriate explanation may be that $K_{drug}$for the (VE/gliadins nanoparticles/decane) system is lower than for the (BZC/gliadins nanoparticles/water) system.

In the literature, the all-*trans*-retinoic acid (RA) release has been observed from gliadins nanoparticles (Ezpelleta et al., 1996), in 100 ml of PBS at pH 7.4 with 15 mg of gliadins nanoparticles containing 60 RA μg gliadins mg^{-1}. A similar two steps profile is observed. The first 20% is released by a burst effect. After the third hour, a slower release takes place. Ezpelleta et al. (1996) had supposed that the phenomenon is ruled by a diffusion process. After 3 h, a similar amount of vitamins (RA and VE) is released by gliadins nanoparticles: around 20% for RA and 25% for VE, even if the conditions of temperature and of drug/release medium are not identical.

4. Conclusion

In conclusion, by a desolvatation method, drug loaded gliadins nanoparticles are obtained with a mean radius about 450–475 nm. Three drugs of different polarity: hydrophobic Vitamin E, slightly polar aromatic mixture and amphiphilic cationic benzalkonium chloride were entrapped in the nanoparticles. The closer the drug and gliadins polarity, the better the drug entrapment. The release from loaded particles, of Vitamin E and of benzalkonium chloride, has been studied and interpreted as a burst effect completed by a drug diffusion process through the particle modelled as a homogenous sphere. The diffusion coefficients of the two drugs measured during the release are of several decades much smaller than in pure liquids. This confirms the strong entrapment of the drug in the nanoparticles.

These results show that the gliadins nanoparticles are suitable controlled released systems for hydrophobic and amphiphilic drugs.

Acknowledgements

Authors are indebted to the “Réseau Matériaux, Polymères, Plasturgie” (Basse Normandie—Haute Normandie, France) for financial support.

References

Alonso, M.J., 1996. Nanoparticulate drug carrier technology. Drug Pharm. Sci. 77, 203–242.

Aubeny, E., Colau, J.C., Nandeuil, A., 2000. Local spermicidal contraception: a comparative study of the acceptability and safety of a new pharmaceutical formulation of benzalkonium chloride, the vaginal capsule, with a reference formulation, the pessary. Eur. J. Contracept. Health Care 5, 61–67.

Barton, A.F.M., 1991. Handbook of Solubility Parameters and Other Cohesion Parameters, 2nd ed. CRC Press, Boca Raton.

Bigelow, C.C., 1967. On the average hydrophobicity of proteins and the relation between it and protein structure. J. Theor. Biol. 16, 187–221.

Chasin, M., Langer, R., 1990. Biodegradable Polymers as Drug Delivery Systems, Marcel Dekker, New York.

Dhillon, A.S., Winterfield, R.W., Thacker, H.L., 1982. Quaternary ammonium compound toxicity in chickens. Avian Dis. 26, 928–931.

Duclairoir, C., Nakache, E., Marchais, H., Orecchioni, A.M., 1998. Formation of gliadin nanoparticles: influence of the solubility parameter of protein solvent. Colloid Polym. Sci. 276, 321–327.

Duclairoir, C., Irache, J.M., Nakache, E., Orecchioni, A.M., Chabenat, C., Popineau, Y., 1999. Gliadin nanoparticles: formation, all-trans-retinoic acid entrapment and release, size optimization. Polym. Int. 79, 327–333.

Epstein, J.H., 1983. Photocarcinogenesis, skincancer and aging. J. Am. Acad. Dermatol. 9, 487–502.

Ezpelleta, I., Irache, J.M., Stainmesse, S., Chabenat, C., Gueguen, J., Popineau, Y., Orecchioni, A.M., 1996. Gliadin nanoparticles for the controlled release of all-*trans*-retinoic acid. Int. J. Pharm. 131, 191–200.

Guy, R.H., Hadgraft, J., Kellaway, I.W., Taylor, M.J., 1982. Calculations of drug release rates from spherical particles. Int. J. Pharm. 11, 109–207.

Hunter, R.J., 1981. Zeta Potential in Colloid Science: Principles and Applications, Academic Press, London.

Idson, B., 1992. Dry skin moisturizing and emolliency. Cosm. Toil. 107, 69–78.

Kagan, V., Witt, E., Goldman, R., Scita, G., Packer, L., 1992. Ultraviolet light induced generation of vitamin E radicals and their recycling. A possible photosensitizing effect of vitamin E in the skin. Free Radic. Res. Comm. 16, 51–54.

Koga, T., Terao, J., 1996. Antioxidant behaviours of vitamin E analogues in unilamellar vesicles. Biosci. Biotechnol. Biochem. 60, 1043–1045.

Larré, C., Popineau, Y., Loisel, W., 1991. Fractionation of gliadins from common wheat by cation exchange FPLC. Cereal Chem. 14, 231–241.

Lis-Balchin, M., Hart, S., 1999. Studies on the mode of action of the essential oil of lavender (*Lavandula angustifolia* P. Miller). PTR Phytother. Res. 13, 540–542.

Marty, J.P., 1998. Vitamins and Skin Aging. Intensive Course in Dermato-cosmetic Sciences, Vrije Universiteit Brussel, Brussels, pp. 115–140.

Marty, J.P., Wepierre, J., 1994. Percutaneous absorption of cosmetics: implication in safety and efficacy. In: Baran, R., Maibach, H.I. (Eds.), Cosmetic Dermatology, Martin Dunitz Ltd., London, UK.

Maryott, A.A., Smith, E.R., 1951. Table of Dielectric Constants. In Circular 514, National Bureau of Standards, New York.

Mayer, P., Pittermann, W., Wallat, S., 1993. The effects of Vitamin E on the skin. Cosm. Toil. 108, 99–109.

Mersmann, A., 1994. Crystallization Technology Handbook, Marcel Dekker, New York.

Nakache, E., Poulain, N., Candau, F., Orecchioni, A.-M., Irache, J.M., 2000. In: Nalwa, H.S. (Ed.), Handbook of Nanostrutured Materials and Nanotechnology, Academic Press, New York.

Patterson, T.F., 1956. Am. Rev. Tub. 74, 284–288.

Popineau, Y., Denery-Papin, S., 1995. Protéines de réserve du grain de blé. In: Godon, B. (Ed.), Protéines végétales, Lavoisier (collection sciences et techniques agro-alimentaires), Londres, New York, Paris, pp. 120–172.

Psychoyos, A., Creatsas, G., Hassan, E., Georgoulias, V., Gravanis, A., 1993. Spermicidal and antiviral properties of cholic acid: contraceptive efficacy of a new marginal sponge (Protectaid) containing sodium chlorate. Hum. Reprod. 8, 866–869.

Sober, A.J., 1987. Solar exposure in the etiology of cutaneous melanoma. Photodermatology 4, 23–31.

Stainmesse, S., Orecchioni, A.-M., Nakache, E., Puisieux, F., Fessi, H., 1995. Formation and stabilization of a biodegradable polymeric colloidal suspension of nanoparticles. Colloid. Polym. Sci. 273, 505–511.

Tamburic, S., Abamba, G., Ryan, J., 1999. Moisturizing potential of D-α-tocopherol. Cosm. Toil. 114, 73–82.

Teglia, A., Secchi, G., 1994. New protein ingredients for skin detergency: relative wheat protein–surfactant complexes. Int. J. Cosmet. Sci. 16, 235–246.

Thies, C. 1996. A survey of microencapsulation processes. In: Benita, S. (Ed.), Microencapsulation: Methods and Industrial Applications. Marcel Dekker, New York, pp. 1–20.

Wainberg, M.A., Spira, B., Bleau, G., Thomas, R., 1990. Inactivation of human immunodeficiency virus type 1 in tissue culture fluid and in genital secretion by the spermicide benzalkonium chloride. J. Clin. Microbiol. 28, 156–158.

Washington, C., 1996. Drug release from microparticulate systems. In: Benita, S. (Ed.), Microencapsulation: Methods and Industrial Applications. Marcel Dekker, New York, pp. 155–181.

Wester, R.C., Maibach, H.I., 1997. Absorption of tocopherol into and through human skin. Cosm. Toil. 112, 53–57.